Time resolved spectroscopic investigation of SiD2 + D2: kinetic study

Time resolved spectroscopic investigation of SiD_2 + D_2: kinetic study

Najem A. Al-Rubaiey[1,*], *Robin* Walsh[2]

[1]Petroleum Technology Department, University of Technology, P.O. Box 35109, Baghdad, Iraq
[2]Chemistry Department, University of Reading, Reading, UK

Abstract. Silylenes (silanediyls) have made an important impact on organosilicon chemistry even if it is of more recent foundation than carbenes in organic chemistry and much less complete. These species are highly reactive intermediates. They play a central role in the chemical vapour deposition (CVD) of various silicon-containing thin films which have a technological importance in microelectronics as well as in the dry etching processes of silicon wafers. Spectroscopic methods have been developed to observe these species, a necessary pre-requisite to their direct monitoring. In this work, deuterated phenylsilane precursor, $PhSiD_3$ was chosen for SiD_2 because its analogue phenylsilane, $PhSiH_3$ proved to be a good precursor for SiH_2 and the high quality decay signals observed revealed that SiD_2 be readily detected from $PhSiD_3$ and that if other decomposition pathways (e.g. PhSiD + D_2) are occurring, they do not effect measurements of the rate constants for SiD_2. The absorption spectrum of SiD_2 formed from the flash photolysis of a mixture of $PhSiD_3$ and SF_6 at 193nm were found in the region 17384-17391 cm^{-1} with strong band at 17387.07 cm^{-1}. This single rotational line of $^pQ_1$ was chosen to monitor SiD_2 removal. Time-resolved studies of SiD_2 have been carried out to obtain rate constants for its bimolecular reactions with D_2. The reactions were studied over the pressure range 5-100 Torr (in SF_6 bath gas) at four temperatures in the range 298-498K. Single decay from 10 photolysis laser shots were averaged and found to give reasonable first-order kinetics fits. Second order kinetics were obtained by pressure dependence of the pseudo first order decay constants and substance D_2 pressures within experimental error. The reaction was found to be weakly pressure dependent at all temperatures, consistent with a third-body mediated association process. In addition, SiH_2+ H_2 reaction is approximately ca. 60% faster than SiD_2+D_2 reaction. Theoretical extrapolations (using Lindemann-Hinshelwood model and Rice, Ramsperger, Kassel and Marcus (RRKM) theory) were also carried out and obtained data fitted the Arrhenius equations.

1 Introduction

The desire to understand the mechanistic details of the reactions of silylene, SiH_2 prompted us to extend our studies to include isotope effect experiments.[1,2]. The only kinetic information available for deuterated silylene, SiD_2 was that for the reaction with H_2. Mason *et al.*[3] reported a rate constant of $3.8\pm0.2\times10^{-12}$ $cm^3molecule^{-1}s^{-1}$ at 5 Torr total pressure in which the reaction found to be pressure independent in the range 2-100 Torr. The possibility of studies with SiD_2 offers the opportunity to give new insights into reaction system previously studied with SiH_2.

For the reaction of SiH_2 with D_2 at room temperature,Jasinski reported a rate constant of 2.6×10^{-12} $cm^3molecule^{-1}s^{-1}$[4]. This was the first reported measurement for this reaction. It compares with a value of 3.2×10^{-12} $cm^3molecule^{-1}s^{-1}$ for the rate constant for the reaction of SiH_2+H_2 obtained by extrapolation to infinite pressure of a pressure dependent process[5,6]. These high values suggest only a small isotope effect and that the energy barrier to insertion was ≤ 1 kcal mol^{-1} [4], this provides experimental support for the higher values of heat of formation at room temperature. This suggestion has been supported by *ab initio* calculations carried out by Gordon and Gano[7]. The calculations for the potential energy surface of the silylene reaction with hydrogen gave an activation energy of 1.7 kcal mol^{-1}.

Subsequently Baggott *et al.*[8] extended Jasinski's room temperature study to cover a range of 298-333K and found k to be in good agreement with Jasinski's reported value[4,5]. The authors found an almost temperature independent rate constants of 1.88×10^{-12} $cm^3molecule^{-1}s^{-1}$. The uncertainties in the rate constants were *ca.* 7%. This indicated that any activation energy was very small and certainly <1.57 kcal mol^{-1}. A slightly negative activation energy cannot be ruled out.

In this work we report the first kinetic studies for the reaction of SiD_2 + D_2 at a wide range of pressures and temperatures. Kinetic studies of SiD_2 are of particular interest in two respects, *viz*

(i) a comparison with SiH_2 data will help elucidate reaction mechanisms,

(ii) many SiH_2 reactions exhibit pressure dependence often making it problematical to obtain high pressure

* Corresponding author: 100108@uotechnology.edu.iq

limiting rate constants. Isotopic scrambling effects make it possible to circumvent this problem with SiD_2 studies.

2 SiD_2 precursor and visible absorption spectrum

$PhSiD_3$ was prepared by reduction of phenyltrichlorosilane ($PhSiCl_3$) with $LiAlD_4$ in dry ether [3]. The prepared $PhSiD_3$ was purified by distillation and found to be 99.8% pure (isotopic purity >92.6%). The $PhSiD_3$ precursor was chosen because its analogue phenylsilane, $PhSiH_3$ proved to be a good precursor for SiH_2. Although SiH_2 formation is not the major product of $PhSiH_3$ photolysis[9], nevertheless, its shown observation, suggest that SiD_2 should be readily detected from $PhSiD_3$. The high quality decay signals observed in the current work reveals that this is true and that if other decomposition pathways (*eg* to PhSiD + D_2) are occurring, they do not effect measurements of the rate constants for SiD_2. A typical averaged decay trace is shown in figure 1.

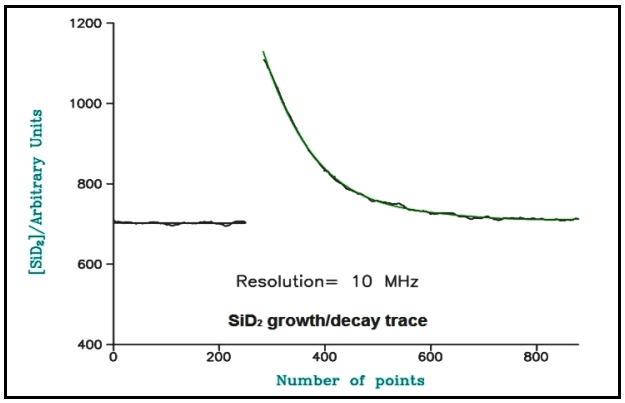

Fig. 1. Typical SiD_2 Absorption trace
(3 mTorr of $PhSiD_3$, 4 Torr D_2 and P_T= 5 Torr in SF_6).

The absorption spectrum of SiD_2, formed from the flash photolysis of a mixture of SiD_4 and D_2, was first investigated by Dubois *et al.* in the region 16175-19200 cm^{-1} [10]. They recorded a visible spectrum of the $(^1B_1)\leftarrow(^1A_1)$ band and found the bending vibrational frequency in the excited state to be 610 nm. However a more detailed spectroscopic study of SiD_2 radicals was reported by other researchers such as Fukushima *et al.* and Muramoto *et al.* [11-13]. Fukushima *et al.* [11] photolysed $PhSiD_3$ at 193nm in the supersonic free jet and observed 11 vibronic bands of the SiD_2 A $(^1B_1) \leftarrow$ X $(^1A_1)$ transition in the wavelength region between 21739.13 and 15625 cm^{-1}.

Because little is known about the SiD_2 radical, any fresh spectroscopic data (as well as kinetic data) are of practical and theoretical interest. Laser spectroscopic investigation of SiD_2 at higher resolution than earlier studies has reached similar conclusions in our lab [3]. Mason *et al.*[3] recorded the absorption spectrum of SiD_2 in the gas phase, using the flash photolysis kinetic absorption technique. SiD_2 was generated by photolysing 10mTorr of $PhSiD_3$ in 5Torr of SF_6 using a series of one-shot photolysis experiments. The authors observed an absorption spectrum in the 17384-17391 cm^{-1} region (the laser linewidth was approximately $3x10^{-5}$ cm^{-1}) with a strong band at 17387.07cm^{-1}, which was attributed to an unknown rotational line $A(^1B_1)(0,3,0)\leftarrow X(^1A_1)(0,0,0)$ vibronic transition of SiD_2. This assignment was based on the original work of Fukushima *et al.*[11]. A 6 cm^{-1} composite spectrum of vibronic transition of SiD_2 is shown in figure 2 (a). Figure 2 (b) also shows the absorption spectrum of SiH_2 for comparison reason. Approximately 8 peaks were displayed for SiD_2 absorption spectrum. The 17387.07 cm^{-1} was found to be the most intense peak. Therefore this peak was chosen to observe the SiD_2 species in this kinetic study. It has been estimated that the intensity of this peak is approximately a quarter of that for the transition used to monitor the SiH_2 species in kinetic studies under similar conditions[3].

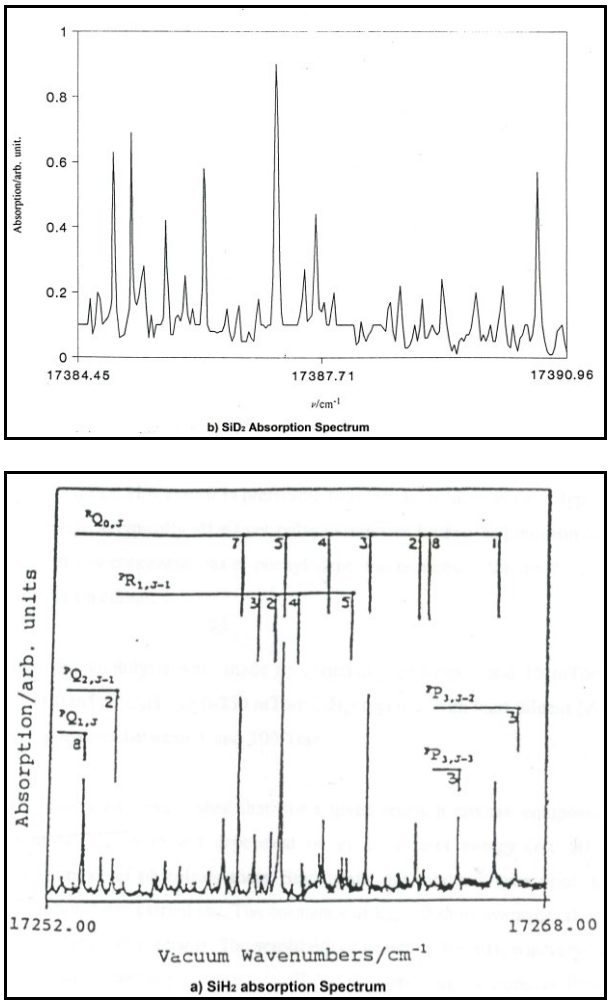

Fig. 2. Absorption spectrum of both a) SiH_2 [4] and b) SiD_2[3].

3 Experimental Setup

Laser flash photolysis/laser absorption apparatus is diagrammatically represented in figure bellow (figure 3).

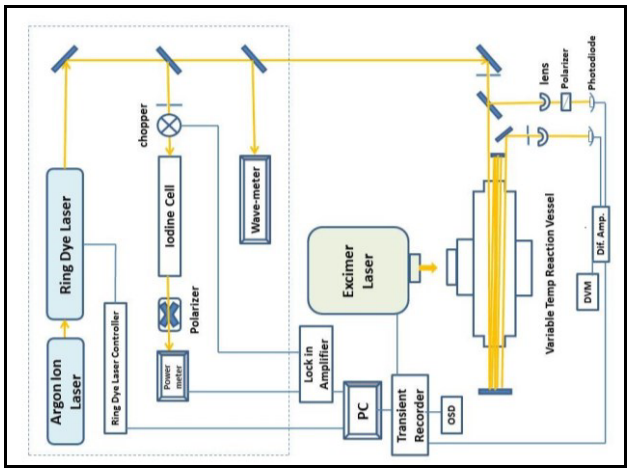

Fig. 3. Schematic diagram of the experimental apparatus.

A mercury-free, glass vacuum line was connected to purpose built variable photolysis cell fitted with a high quality crown glass end windows at Brewster's angle backed by a rotary pump. SiD_2 was produced by the 193 nm flash photolysis of phenylsilane ($PhSiD_3$) using an Oxford KX2, ArF excimer laser. The emitted pulses have 0.1-1J of energy delivered in a 10 ns light pulse with a repetition rate of 1 Hz. SiD_2 concentrations were monitored in real time by means of a Coherent 699–21 single-mode dye laser pumped by an Innova 90–5 Ar^+ laser using Rhodamine 6G in solution as an active medium, which provides tunable radiation in the range 560-610nm. The monitoring laser beam was multipassed between 24-48 times through the reaction zone to give an effective path length of between 0.6-6 m. The monitoring laser was tuned to 17387.07 cm^{-1}. A differential amplifier was connected to two photodiodes and then fed into Datalab Dl910 transient recorder (20 MHz resolution). The transient recorder's external trigger was activated by radiofrequency noise produced when the excimer laser was fired. Traces were observed during runs and interfaced to a computer via a commercial interface (Camplus) where the signal could be displayed and analyzed.

4 Results

The SiD_2 exponential decay curves were recorded and averaged for 10 excimer laser shots. The degree of depletion of the photolysis mixture was negligible. Experiments were carried out with gas mixtures containing a few mTorr of $PhSiD_3$, varying quantities of D_2 up to 9.5 Torr, and inert diluent bath gas (SF_6) at total pressures from 5 to 100 Torr to test for pressure dependence. For each pressure, a series of runs (7 points) was performed at different substrate concentrations, as been illustrated in figure 4.

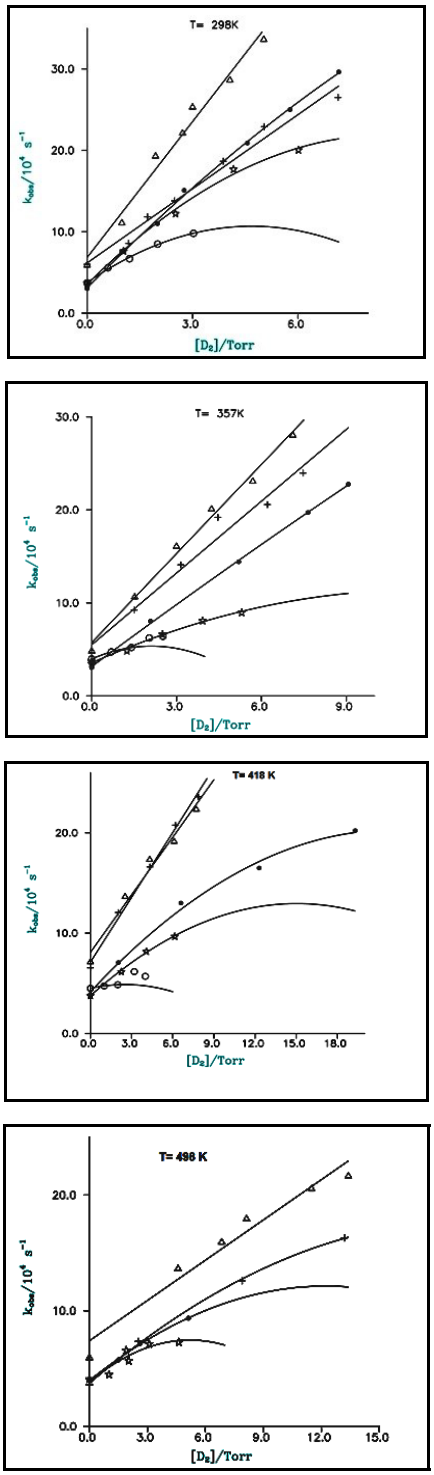

Fig. 4. Second-order plots for the reaction of SiD_2 + D_2 at various total pressures (in SF_6) and Temperatures.
❍, 5; ★, 10; •, 20; +, 50; Δ, 100 Torr.

Only second order plots for data recorded at a total pressure above 20 Torr in SF_6 were linear. Plots for total pressures below this were curved. The quadratic procedure using the polynomial regression was applied for these cases in order to obtain the second order rate constants as gradients of the plots. The intercept corresponds to loss of silylene in the absence of substrate i.e. by reaction with $PhSiD_3$. The correlation of fitting constants means that the rate constants are somewhat less reliable by this procedure.
Second order rate constants were calculated using the following expression:

$$k(cm^3\ \text{molecule}^{-1}s^{-1}) = \frac{Gradient(Torr^{-1}\ s^{-1}) \times T(K)}{F}$$

The conversion factor, F, was obtained from the ideal gas equation (PV=nRT where R=8.3145 J $K^{-1}mol^{-1}$). Its value is F= 9.657×10^{18}.

The second order rate constants for these experiments, representing over 100 measurements of individual rate constants are shown in figure 5 and listed in table 1.

The uncertainties in individual second order rate constants are about *ca.* ± 20% for total pressures <20 Torr and ± 10% for total pressure >20 Torr, but are not shown in the figures to avoid complicating them.

Table.1 Absolute rate constants for the reaction of SiD_2 + D_2

P/Torr	k/10^{-12} $cm^3molecule^{-1}s^{-1}$			
	298K	357K	418K	498K
5	0.91±0.1	0.45±0.1	0.23±0.1	-
10	1.33±0.1	0.53±0.1	0.53±0.1	-
20	1.35±0.1	0.83±0.1	0.63±0.1	0.69±0.2
50	1.21±0.2	1.16±0.2	1.04±0.1	0.66±0.2
100	1.72±0.2	1.36±0.2	1.00±0.1	0.78±0.2

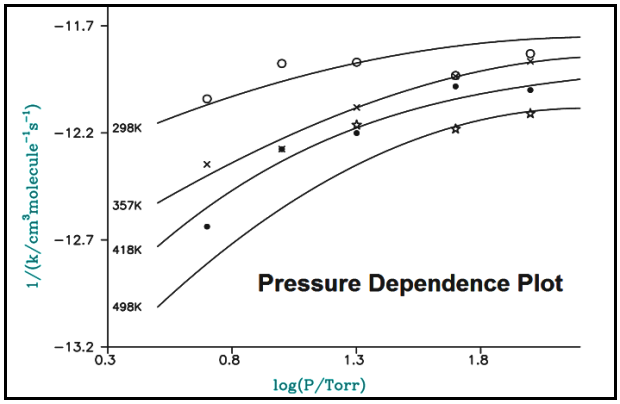

Fig.5. Pressure dependence of second-order rate constants for SiD_2 + D_2 at different temperatures in SF_6 buffer gas.

Comparison of absolute rate constants can only be made at 300K between the reactions of SiH_2+H_2 and SiD_2+D_2 due to big differences of temperatures used in these studies, see figure 6. The graph shows that the SiH_2+ H_2 reaction is approximately ca. 60% faster than SiD_2+D_2 reaction at high pressure.

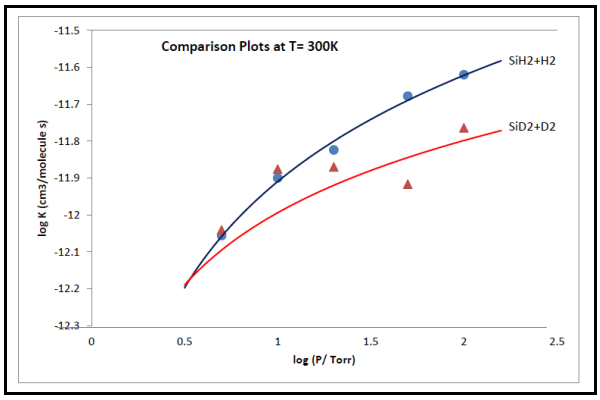

Fig.6. Pressure dependence of second-order rate constants for SiH_2+H_2 and SiD_2+D_2 at T=300K.

The measured rate constants demonstrate the reaction is relatively slow and rate constants are weakly pressure dependent at all temperatures, consistent with a third-body mediated association process. In addition, SiH_2+ H_2 reaction is approximately ca. 60-70% faster than SiD_2+D_2 reaction at higher total pressure.

5 Extrapolation by empirical procedures

Since SiD_2+D_2 study lies in the fall-off region at accessible pressures, a reliable method of extrapolation to infinite pressure must be employed. A number of methods have been suggested and used by various workers.

The earliest extrapolation procedure employed plots of k^{-1} versus P^{-1}. This plot follows from the Hinshelwood-Lindemann model. Recently Oref and Rabinovitch[14] have suggested another empirical procedure which theoretically should yield more accurate infinite pressure rate constants since the precise nature of the extrapolation is determined by the actual data. They suggest a plot of k^{-1} versus P^{α} where α lies between 0 and 1 and is optimised to give the best linear plot. Values of α on either side of the optimum value will give curved plots which would lead to an overestimate and underestimate of k^{∞} resp. It is important to state that there is no absolute theoretical justification for either of the methods described above. They are simply empirical procedures which have been found to give reasonable linear plots. In the present work the latter method of extrapolation (where α= 0.5 and 1) has been tried and the results are compared.

When data are only available at pressures well into the fall off region it becomes clear that the choice of method of extrapolation becomes crucial, since different methods give different answers. In the current work it was extremely difficult to judge the quality of the fits because of data scatter, values of k^{∞} (represented by $(\text{intercept})^{-1}$) had a large uncertainty. Therefore a modified procedure was adopted here in which a number of points were selected from interpolated curves (drawn by hand). These interpolated fall-off curves were used to represent the data in order to obtain k^{∞} with minimum error (see figure 7).

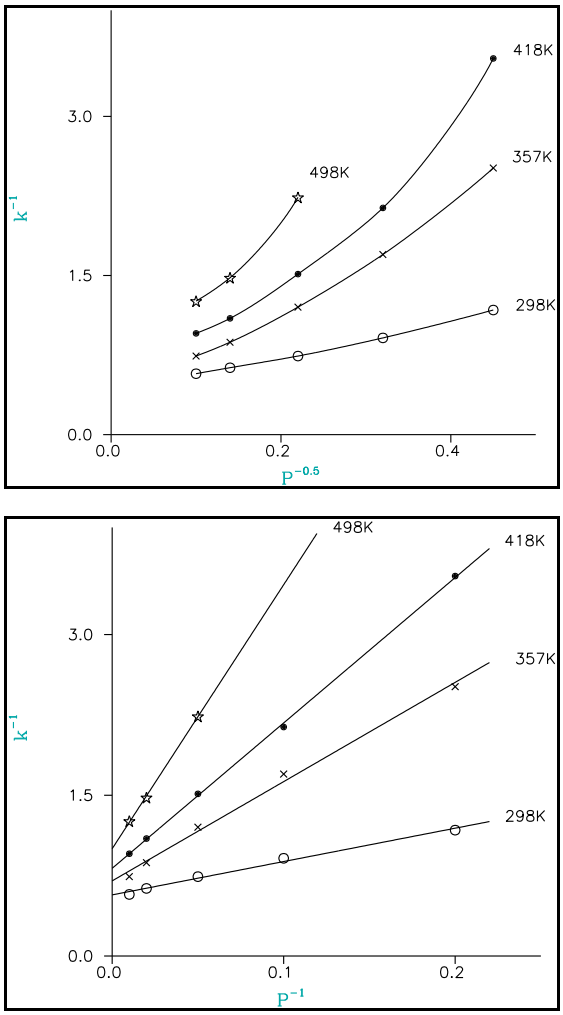

Fig.7. Empirical procedure for $SiD_2 + D_2$.

We find that the plot is not absolutely linear. Consequently some error in the infinite pressure rate constants obtained using a least-squares line must be expected. If we consider the k^{-1} versus $P^{-0.5}$ we find that such plots suffer from marked curvature making extrapolation difficult and leading to an underestimated of k^{∞}. On the other hand the k^{-1} versus P^{-1} plots are much less curved. It must be noted, however, that scatter in the experimental data can make calculation of an optimum α difficult and may limit the applicability of this method.

The temperature dependence for the reaction may be expressed in Arrhenius form. The derived Arrhenius parameters are shown in table 5. Figure 8 shows a graph of the Arrhenius plot for both SiH_2+H_2 [15] and SiD_2+D_2 reactions. These data show a number of interesting features. First the reaction has a negative activation energies E= - 0.82±0.05 kcal mol^{-1}. Secondly there is a significant difference between SiH_2+H_2 and SiD_2+D_2. The former reaction is ca. 60% faster than the latter.

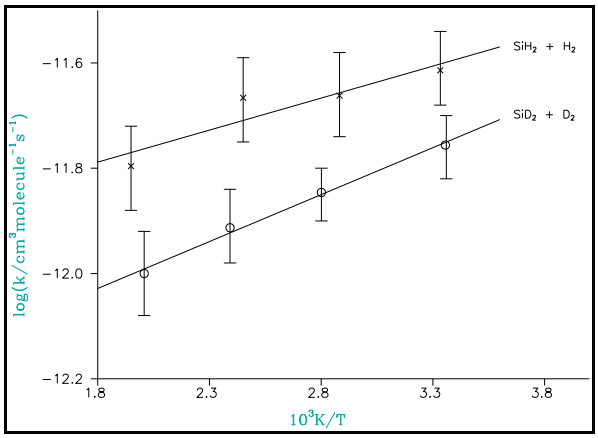

Fig.8. Arrhenius plots for x, SiH_2+H_2 [23]; O, SiD_2+D_2.

6 RRKM modelling of experiments

In order to try to fit the observed pressure dependence of the insertion of $SiD_2 + D_2$, RRKM calculations were carried out on the pressure dependence of the inverse silane, SiD_4 decomposition in the conventional manner.

$\langle\Delta E\rangle_{down}$ were based on the assumption of a fixed energy removed on each collision (stepladder model). However we did not include some other correction factors (eg F_{rot}) which could have some effect. For a small molecule like silane (highly excited), the anharmonicity effect was found to be important[16,17]. This correction factor influences the density of states of the reactant at an internal energy equal to the critical energy. The low pressure limiting rate constant is proportional to the anharmonicity factor, by increasing the value of this factor better agreement with the data was obtained [17-19]. It has been suggested that increasing the value of this factor has roughly the same effect as increasing the "looseness" of the transition state.

The fall-off predictions are very sensitive to some of the parameters and not very sensitive to others. The exact assignments of reactant frequencies, transition state frequencies, and reactant path degeneracy are not very important as long as these assignments reproduce the required high pressure A-factor. On the other hand, assignment of bath gas collision efficiencies and their temperature dependencies can be very important, particularly when the reaction is well into its pressure-dependent region and the bath gas molecules are weak colliders.

The effect of varying the energy level grain size (GRAIN) is rather unpredictable and its choice affects the position of the fall-off curves for both strong and weak collision situations. This parameter is used to define the energy gap in the quasi-quantised energy scale covering the energy range of interest. It is clear that the smaller its value, the more closely packed are the levels. Therefore in principle smaller grain sizes are best (although this increases the size of programme storage required and decreases the speed of calculations). However the calculation is also sensitive to the positioning of the critical energy, E_o with the quantised energy levels. The best situation appears to be when E_o

lies in the center of a grain. The choice of minimum energy value, E_{min} and grain size, determines this. In practice there were chosen to get closer to this condition. The energy range starts from just below the initial energy and goes up to 2-3 times its value. In the present calculation for silylene reaction with hydrogen this parameter was set to be 50 cm^{-1}. The vibration frequencies assigned to the SiD_4 complex were based on those from ab initio calculations of Gordon et al.[20]. The details of the model and parameters used are shown in tables 2, and 3.

Table 2. RRKM parameters for SiD_4 decomposition model, predicted by Gordon *et al.*[20]

	SiD_4	SiD_4^+
	1597(3) 1558(1) 701(2) 681(3)	1579(1) 1551(1) 1488(1) 1163(1) 721(1) 681(1) 528(1) 498(1)
I_i/amu A^2	11.777 11.777 11.776	13.685 11.558 9.707
Path degeneracy	12	
Reaction coordinate	681	
E_o/ kcal mol^{-1}	56.18 (298K)	
log(A/s^{-1})	14.38 (298K)	
Z_{LJ}/ 10^{-10} cm^3 $molec^{-1}$ s^{-1}	4.354 (SF_6, 298K)	

Table 3. Z_{LJ} for SiD_4 decomposition.

Temperature/K	$Z_{LJ}/10^{-10}$ $cm^3 molecule^{-1} s^{-1}$
298	4.354
357	4.487
418	4.620
498	4.785

The A-factors used here are those obtained using the vibration wavenumbers for both the molecule and the Transition State (employing Smol programme) [15]. Since both SiH_4 and SiD_4 have the same electronic energies, the critical energies can be obtained from the standard formula ($E_o=E_{el}+\Delta zpe$). Δzpe is defined as the difference between the zero-point energies of the reactant and activated complex. The activation energies then can be calculated using the equation $E_a = E_o + RT + \langle E^+ \rangle - \langle E \rangle$. The results of these calculations are shown in table 4.

Table 4. Activation energies and A-factors for SiD_4 decomposition.

T/K	log(A/s^{-1})	E_a/kcal mol^{-1}	E_o/kcal mol^{-1}
298	14.38	56.83	56.18
357	14.45	56.80	56.04
418	14.51	56.74	55.87
498	14.57	56.64	55.65

The calculations were carried out using both a strong and a weak collision model to generate fall-off curves at four different temperatures. A weak collision ($\langle \Delta E \rangle_{down}$= 2.3 kcal mol^{-1}) was fixed to fit the rate constants at all four temperatures and is reasonably consistent with collisional efficiencies found with similar systems[20]. However these calculations were carried out without including the F_{an} factor which was assumed to have a small effect.

The results are plotted in figure 9 with experimentally determined rate constants. The high pressure limit rate constants were derived from the isotope effect calculations combined with $SiH_2 + D_2$ rate data[15]. Reasonable agreement was obtained with the data when compared to that of the previous reaction, except for T=357K where the theoretical fit and data were in disagreement. However there are probably other choices of parameters that would have produced equally good fits.

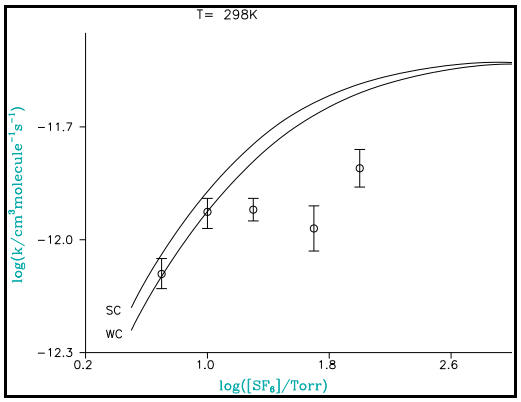

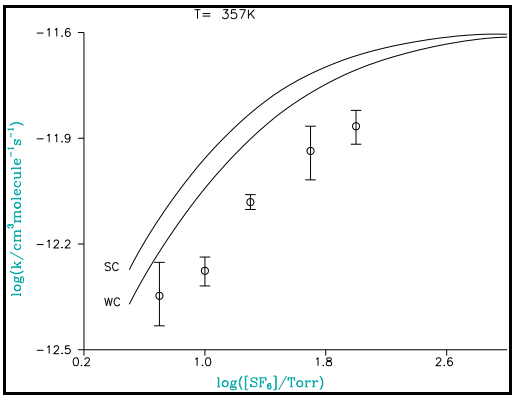

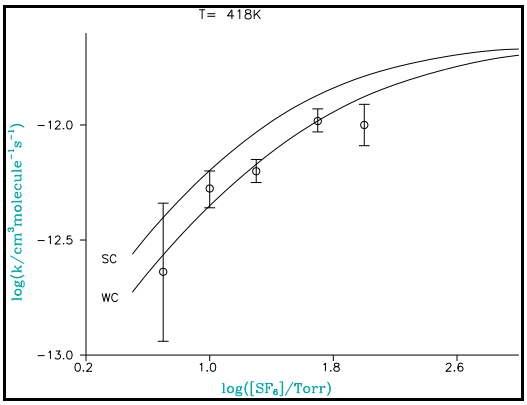

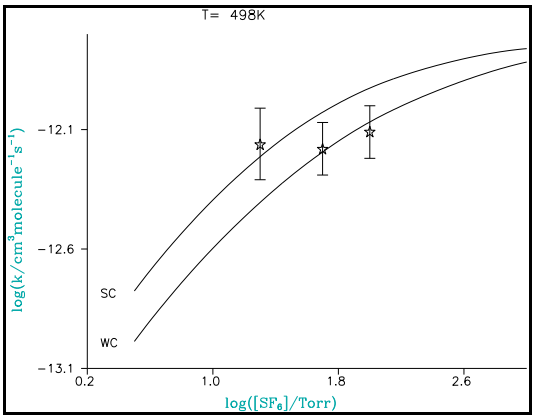

Fig.9. Pressure dependence of second-order rate constants for $SiD_2 + D_2$ at different temperatures in SF_6 buffer gas (solid lines are RRKM fits). sc, Strong collision; wc, Weak collision

7 Discussion

These studies proved to be more difficult than earlier ones for silylene with olefins[21]. This arose because the rate constants were smaller and a significant amount of hydrogen was required to observe a reaction. This meant that at low total pressures, reaction of silylene with precursor was always a substantial fraction of the total decay. The magnitude of the intercept of the second order plots were kept as small as possible. This was done by reducing the partial pressure of SiD_4 to the minimum consistent with signal to noise constraints.

This restricted the range of possible substrate pressures and temperatures over which reactions could be studied. At high partial pressures of hydrogen necessary to obtain reaction, SF_6 is present in insufficient quantity to ensure that it is the dominant bath gas collider. This causes curvature in the second order plots (at fixed total pressures). By using a polynomial procedure (quadratic), we are assuming that the slope at $[D_2/Torr]=0$ will provide a reliable estimate of the first-order rate coefficients, k_{obs}, for the removal of SiD_2 in the presence of hydrogen. However this leads to higher uncertainties in this case compared to those of other studies (*eg* $SiH_2 + C_2H_4$)[21].

A high pressure limit rate comparison is shown in table 5 using different extrapolation procedures.

Table 5. High pressure limit rate comparison for the reaction of $SiD_2 + D_2$ using three different procedures.

T/K	$k^\infty/10^{-12}$ cm^3 molecule^{-1} s^{-1}		
	RRKM	**Empirical Procedure**	**Isotope Effect**
298	2.24	1.75 ± 0.35	3.38
357	1.78	1.43 ± 0.29	2.54
418	1.58	1.22 ± 0.24	2.23
498	1.41	1.00 ± 0.20	1.92

A comparison is also made for the activation energies and the A-factors for silylene reaction with hydrogen and its isotopic analogues in table 6 (obtained from extrapolation of experimental data to the high pressure limit using empirical procedure).

Table 6. Arrhenius parameters for SiH_2+H_2 and isotopic variants

Reaction	log (A/ cm^{3}molec^{-1}s^{-1})	Activation energy kJ mol^{-1}
$SiH_2 + H_2$	-12.01[a] -11.75[b]	-2.34 -1.84
$SiD_2 + D_2$	-12.35[a] -12.09[b]	-3.41 -3.52
$SiH_2 + D_2$	-12.07[c]	-2.03
$SiD_2 + H_2$	-11.87[d]	-2.54

[a]. Obtained by extrapolation (empirical procedure) [15]
[b]. Based on isotope effect calculations[15]
[c]. P_T= 10 Torr[15], [d]. P_T= 10 Torr[3]

The following figures can be drawn from this table. Arrhenius parameters of E_a= -0.48 ± 0.33 kcal mol^{-1} and A-factor= $0.80\pm0.35\times10^{-12}$ cm^{3}molecule^{-1}s^{-1} can be averaged. The activation energy for the reaction (SiH_2+H_2) is approximately a factor of 1.5 smaller than that obtained from reaction (SiD_2+D_2) by extrapolation to the high pressure limit.

A reasonable agreement was seen between theory and experiment for SiD_4 decomposition. However there are probably other choices of parameters that would have produced equally good fits. Parameters such as the average energy removal, $\langle\Delta E\rangle_{down}$, and the high pressure limit rate constant, k^∞, can be adjusted to obtain a better fit (see table 5).

An example is shown in figure 10 at T= 357K, which shows the fall-off curve when $\langle\Delta E\rangle_{down}$= 2.3 kcal mol^{-1} and k^∞= 1.78 x 10^{-12} cm^{3}molecule^{-1}s^{-1}.

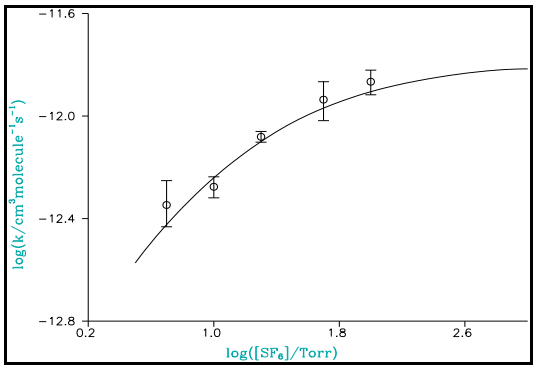

Fig. 10. Pressure dependence of second-order rate constants for $SiD_2 + D_2$ at T= 357K (solid line is RRKM fit)

8 Summary and future work

Time-resolved study of SiD_2 generated by laser flash photolysis of ($PhSiD_3$) has been carried out to obtain rate constants for its bimolecular reactions with D_2. The reaction was studied over the pressure range 5-100 Torr (in SF_6 bath gas) at four temperatures in the range 298-498K. The reaction was found to be pressure dependent at all temperatures, consistent with a third-body mediated association process. The reactions were modelled using empirical and theoretical procedures to obtain the high pressure limit rate constants. The empirical procedure employed the Hinshelwood-Lindemann model. The data obtained using these extrapolations were fitted to the Arrhenius equation. RRKM modelling, based on the transition states (SiD_4) of Gordon *et al*, gave a reasonable fit to the experiments. Further work is required in the following areas; (i) the RRKM calculation described in this work can be improved by considering some other correction factors in addition to that of F_{an}. (ii) the pressure dependence of the pyrolysis of silane also needs to be reinvestigated over a wider pressure range in order to obtain an improved value for k^{∞} for $SiD_4 \rightarrow SiD_2 + D_2$. This would then improve the value for the heat of formation of silylene.

References

1. N Al-Rubaiey, HM Frey, BP Mason, C McMahon, R Walsh, Chem. Phys. Lett., **203**, (3-4), 301-305 (1993).
2. N Al-Rubaiey, IW Carpenter, R Walsh, R Becerra, Mark S Gordon, The Journal of Phys. Chem. B, **102** (44), 8564-8572 (1998).
3. B.P Mason, H.M. Frey, and R. Walsh, J. Chem. Soc. Faraday Trans., **89**, 4405 (1993).
4. J.M. Jasinski, J. Phys. Chem., , **90**, 555 (1986).
5. J.M. Jasinski, J.O. Chu, in "Silicon Chemistry", ed. by J.Y. Corey, E.R. Corey, and P.P. Gaspar, Ellis Horwood, Chichester, UK, (1988).
6. J.M. Jasinski, J.O. Chu, J. Chem. Phys., **88**, 1678 (1988).
7. M.S. Gordon, D.R. Gano, J.S. Binkley, M.J. Frisch, J. Am. Chem. Soc., **108**, 2191 (1986).
8. J.E. Baggott, H.M. Frey, K.D. King, P.D. Lightfoot, R. Walsh, I.M. Watts, J. Phys. Chem., **92**, 4025 (1988).
9. J.E. Baggott, H.M. Frey, P.D. Lightfoot, R. Walsh, Chem. Phys. Lett, **22**, 125 (1986).
10. I. Dubois, G. Herzberg, R. D. Verma, J. Chem. Phys., **47**, 4262 (1967).
11. M. Fukushima, S. Mayama, K. Obi, J. Chem. Phys., **96**, 44 (1992).
12. Fukushima, M.; Obi, K., , J. Chem. Phys., **100**, 9, 6221 (1994)
13. Muramoto, Y.; Ishikawa, H., J. Chem. Phys., **122**, 15, 154302 (2005).
14. I. Oref and B.S. Rabinovitch, J. Phys. Chem., **72** (13), 4488 (1968).
15. N. Al-Rubaye and R. Walsh, to be published.
16. J. Troe, J. Phys. Chem., **83**, 114 (1979).
17. K.F. Roenigk, K.F. Jensen, and R.W. Carr, J. Phys. Chem., **91**, 5736 (1987).
18. H.K. Moffat, K.F. Jensen, R.W. Carr, J. Phys. Chem., **95**, 145 (1991).
19. J.M. Jasinski and J.O. Chu, J. Chem. Phys., **88**, 71678 (1988).
20. M.S. Gordon, private communications to R. Walsh.
21. N. Al-Rubaiey and R. Walsh, J. Phys. Chem., **98** (20), 5303 (1994).